TC-1 observations of flux pileup and dipolarization-associated expansion in the near-Earth magnetotail during substorms

H. Zhang,[1] Z. Y. Pu,[1,2] X. Cao,[1] S. Y. Fu,[1] Z. X. Liu,[2] Z. W. Ma,[3] M. W. Dunlop,[4] W. Baumjohann,[5] C. J. Xiao,[6] M. H. Hong,[7] J. B. Cao,[2] Q. G. Zong,[8] X. G. Wang,[9] C. Carr,[10] H. A. Rème,[11] I. Dandouras,[11] A. Fazakerley,[12] H. U. Frey,[13] and C. P. Escoubet[14]

Received 29 September 2006; revised 13 November 2006; accepted 12 December 2006; published 3 February 2007.

[1] Fifty-three substorms measured by Double Star/TC-1 in the near-Earth magnetotail from July to October, 2004 are studied. The main features of these events are: (a) Magnetic flux pileup characterized by continuous enhancement of B_z is observed, which starts almost simultaneously with aurora breakup within 1–3 minutes, indicating that substorm onset is in close relation to flux pileup. (b) Sudden plasma sheet expansion with sharp increases in ion temperature and density is seen in all events, which occurs typically ~11 minutes after the beginning of pileup. The plasma sheet expansion is shown to be in close relation with the primary substorm dipolarization and, hence, can be referred to as 'dipolarization-associated expansion'. (c) Evidence indicates that the substorm current wedge first forms earthward of TC-1 position and, hence, inward of the flow braking region, and then propagates tailward with an expansion in the Z-direction. Possible implications of these observations are briefly discussed. **Citation:** Zhang, H., et al. (2007), TC-1 observations of flux pileup and dipolarization-associated expansion in the near-Earth magnetotail during substorms, *Geophys. Res. Lett.*, *34*, L03104, doi:10.1029/2006GL028326.

1. Introduction

[2] Magnetospheric substorms consist of a chain of processes responsible for the explosive release of the magnetic energy stored in the magnetotail. In the near-Earth neutral line (NENL) model [*McPherron*, 1991], the energy release was thought to be initiated and accomplished through magnetic reconnection (MR) in the mid-tail. On the other hand, the near-Earth current disruption (NECD) model considers that instabilities closer to the Earth lead to current disruption and trigger the substorm expansion phase [*Lui*, 1996]. The occurrence of mid-tail MR has been confirmed after the launch of Geotail [*Nagai et al.*, 1998; *Baumjohann et al.*, 1999]. The NENL paradigm has been improved [*Baker et al.*, 1996] and updated [*Baumjohann*, 2002] since then.

[3] In the updated NENL model, the bursty bulk flows (BBFs) originating from MR between ~20 and ~25 R_E take energy into the inner tail and typically stop outside ~13–15 R_E [*Shiokawa et al.*, 1997]. Magnetic flux then piles up against this boundary, which ultimately leads to a more dipolar tail configuration and, hence, to substorm dipolarization [*Shiokawa et al.*, 1998]. The pressure gradient built up by flow braking causes reduction and diversion of the duskward cross-tail current, forming the substorm current wedge (SCW) [*Birn et al.*, 1999]. This scenario helps to resolve the puzzle that substorm aurora breakup typically maps to the equatorial region near $10R_E$, while near-Earth MR takes place further out [*Baumjohann*, 2002].

[4] During July to October, the apogee of Double Star/TC-1 is about 13 R_E from the Earth in the tail [*Liu et al.*, 2005]. This enables to directly study the substorm initiation with in situ measurements [*Nakamura et al.*, 2006]. From July to October, 2004 TC-1 observed 94 pileup/dipolarization events, which can be divided into two categories: (1) there are 41 events in which increase in B_z and drop of B_x are seen simultaneously, either a few minutes after aurora breakup (majority) or about concurrently with aurora brightening (minority); (2) in another 53 events TC-1 observes that B_z starts to increase almost simultaneously with the aurora breakup, within ~1–3 minutes, and ~11 minutes before the drop of B_x occurs. This paper is devoted to a study of the later type of events. We first conduct a case study of an event on 17 September 2004, then present statistical results of the 53 cases, and finally make discussions and a brief summary.

2. Instrumentations

[5] Data with 4 sec resolution from FGM, HIA and PEACE instruments on board TC-1 are used to investigate

[1]School of Earth and Space Sciences, Peking University, Beijing, China.
[2]Center for Space Science and Applied Research, Chinese Academy of Sciences, Beijing, China.
[3]Department of Physics, Zhejiang University, Hangzhou, China.
[4]Space Sciences Division, Rutherford-Appleton Laboratory, Oxford, UK.
[5]Space Research Institute, Austrian Academy of Sciences, Graz, Austria.
[6]National Astronomical Observatories, Chinese Academy of Sciences, Beijing, China.
[7]Institute of Geology and Geophysics, Chinese Academy of Sciences, Beijing, China.
[8]Center for Atmospheric Research, University of Massachusetts-Lowell, Lowell, Massachusetts, USA.
[9]School of Physics, Peking University, Beijing, China.
[10]The Blackett Laboratory, Imperial College, London, UK.
[11]Centre d'Etudes Spatiale des Rayonnements, Toulouse, France.
[12]Mullard Space Science Laboratory, University College London, Surrey, UK.
[13]Space Science Laboratory, University of California, Berkeley, Berkeley, California, USA.
[14]Solar and Solar Terrestrial Missions Division (SCI-SH), ESA/ESTEC, Noordwijk, Netherlands.

0094-8276/07/2006GL028326

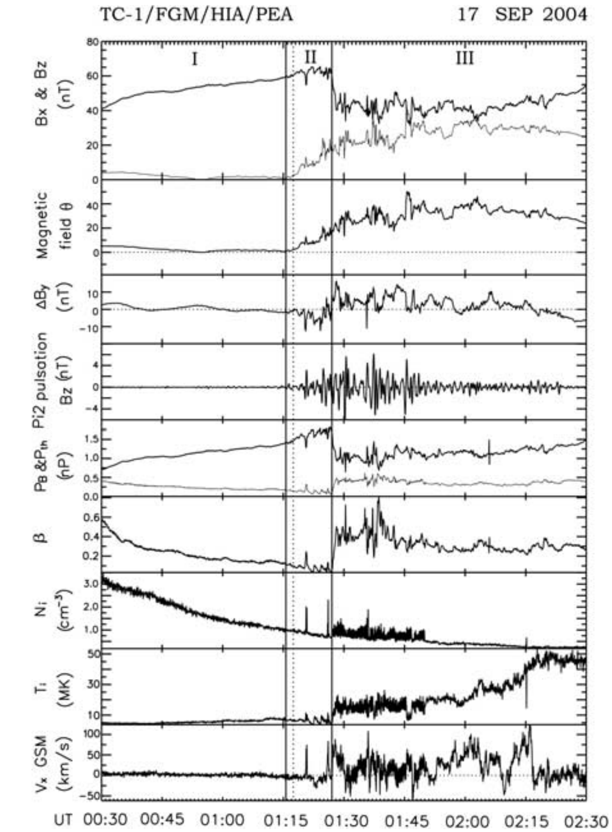

Figure 1. TC-1 measurements of the 17 September 2004 event. From top to bottom are: the B_x (thick) and B_z (thin) component of the magnetic field; the magnetic field elevation angle θ; ΔB_y, the variation of B_y to the background B_{yo} ($\sim$3.6nT); the B_z variations in the Pi2 periods range (40–150 s); the magnetic pressure P_B (thick) and plasma pressure (ions plus electrons) P_{th} (thin); β (the ratio of the plasma pressure to the magnetic pressure); the ion number density N_i; the ion temperature T_i; and the X-component of ion velocity V_x.

the magnetic field and key plasma parameters. The FGM samples the magnetic field vectors [*Carr et al.*, 2005]. The HIA [*Rème et al.*, 2005] and PEACE [*Fazakerley et al.*, 2005] instruments are capable of obtaining full three-dimensional velocity distributions of ions, covering energy ranges from 5 to 32 keV/q, and electrons from 0.7 to 30 keV/q, respectively. The substorm auroral breakup (i.e. the expansion onset) is identified by the aurora observations with a time resolution of 120 sec from IMAGE/WIC, which selects the spectral range between 140 and 160 nm [*Frey et al.*, 2004]. The interplanetary magnetic field (IMF) conditions are monitored by ACE/MAG.

3. Case Study of Substorm on 17 September 2004

3.1. Overview of Observations

[6] Figure 1 shows the TC-1 magnetic field and plasma measurements in GSM coordinates. At $\sim$01:16 UT B_z and B_t (not shown) start to increase, together with the beginning of oscillations of B_z in the Pi2 frequency range. Meanwhile, N_i, P_{th} and β are continuously decreasing. About 11 minutes later at $\sim$01:27 UT, a sharp decrease in B_x appears, along with rapid increases in N_i, T_i, P_{th} and β. Figure 2 displays the sudden auroral brightening observed by IMAGE/WIC, and shows that the substorm expansion onset occurs at $\sim$01:17 UT, which is marked on Figure 1 by the dashed vertical line. During this event, TC-1 was located at (−10.1, −1.4, 1.0)R_E (GSM) at post-midnight, while auroral brightening appeared at pre-midnight ($\sim$20–22 MLT).

3.2. Detailed Analysis

3.2.1. Evolution of Tail Configuration

[7] Evolution of tail configuration can be divided into three stages. Stage I develops from $\sim$00:30 until 01:16 UT, during which time, the elevation angle θ keeps decaying and the magnetotail field becomes more tail-like. The IMF remains southward. The continuous decreases in β and N_i suggest a thinning of the plasma sheet. Stage II lasts from 01:16 until 01:27 UT in which B_z increases and θ rises, for 11 minutes, from 1° up to 20°, while B_x remains basically constant. B_t is enhanced with time in concert with the increase in B_z. Note that during stage II, N_i, P_{th} and β continue to decrease, and TC-1 is sampling boundary layer plasma. Stage III begins with a sudden collapse of B_x from 65 nT to 40 nT at $\sim$01:27 UT along with a slight increase in B_z, which immediately causes the tail to become more dipolar than in stage II. In addition, θ rises rapidly with a jump of 13° from 20° to 33° in $\sim$3 minutes. In the rest of stage III, from about 01:30 to $\sim$02:17 UT, the tail basically remains in this dipolar shape.

3.2.2. Flux Pileup

[8] B_z (and B_t) continuously enhances during the whole of stage II, while B_x keeps nearly constant, indicating a field compression in the X-direction. We refer to this phenomenon as flux pileup. Meanwhile, N_i continues to drop and T_i maintains approximately constant with $T_{i,\perp} > T_{i,\parallel}$ (not shown in Figure 1). As a result, P_{th} and β tend to reduce. About 8 minutes prior to stage II, Cluster at $X \sim -15.1\ R_E$ and $Z \sim 3.7\ R_E$ started to observe an earthward flow with $V_x \approx 300$ km/s on average (not shown in the paper). Since the flow at TC-1 remains small in this interval, it is inferred that the BBF was braking and piled up flux tailward of TC-1. Alternatively, it might also be possible that TC-1 missed the BBF owing to its high position to the plasma sheet. Nevertheless, we prefer to the former. *Shiokawa et al.* [1997] have shown that in most cases BBF was braking and piled up flux tailward of outside $\sim$−13 to −15 R_E. While B_z, B_t and θ are increasing, plasma is possibly squeezed out, N_i, P_{th} and β are then reduced. The phenomenon is similar

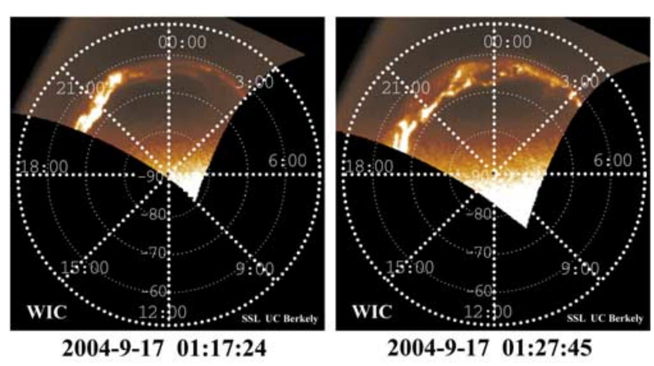

Figure 2. Auroral brightening observed by IMAGE/WIC in the event of 17 September 2004.

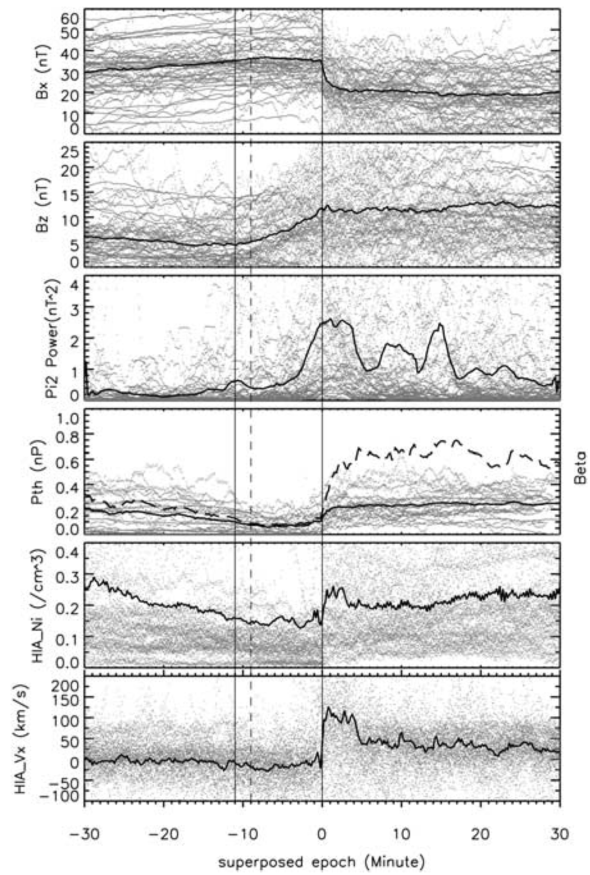

Figure 3. The superposed epoch analysis based on 53 events. From top to bottom are: B_x; B_z; Pi2 wave power in B_z; the plasma pressure P_{th} (solid line) and β (dash line); the ion number density N_i; and V_x, the X-component of ion velocity. The first vertical line (−11 min) marks the average time of aurora breakup, the dash line marks the auroral breakup (−9 min), and the third one (0 min) denotes the beginning of sudden decrease in Bx (DAE).

to the formation of the plasma depletion layer sunward of magnetopause, where particles are squeezed away from the high-magnetic-pressure region as the flux tubes convect toward the magnetopause. In fact, in the inner region of the depletion layer, the flow normal to the magnetopause is almost zero [*Phan et al.*, 1994]. Flow braking may generate fast-mode waves [*Shiokawa et al.*, 1998]. This may be the reason why oscillations of B_z in the Pi2 frequency range begin at the same time when the pileup starts.

3.2.3. Dipolarization-Associated Expansion

[9] We identify the rapid drop of B_x between 01:27 UT and 01:30 UT as dipolarization-associated expansion (DAE) at the TC-1 location. At the very start of the DAE, N_i, T_i, β and P_{th} all suddenly jump up, implying a quick expansion of the plasma sheet. The DAE is observed ~11 (10) minutes after the beginning of flux pileup (aurora breakup). A noticeable variation in B_y is also seen at the DAE. Before ~01:16 UT the background B_{yo} is 3.6 nT. ΔB_y ($B_y - B_{yo}$) turns to be negative at 01:18 UT. A sudden reversal of ΔB_y from negative to positive occurs right at the DAE. Hereafter ΔB_y remains positive. The spacecraft is on the northern dawnside of the plasma sheet. In the frame of the SCW which is symmetric to the Sun-Earth line, negative ΔB_y indicates that the downward field-aligned current (FAC) is located at earthward and equatorward of TC-1, while a positive value implies the opposite. The changing of ΔB_y from negative to positive indicates that the front of the SCW is passing through TC-1 tailward [*Lopez and Lui*, 1990; *Jacquey et al.*, 1991], with an expansion in the Z-direction. This implies that the primary dipolarization occurs initially inside the TC-1 location and moves tailward afterwards, which is consistent with the fact that the DAE is observed ~10 minutes after the aurora breakup. The local plasma sheet expansion at TC-1 is clearly associated with the primary dipolarization, therefore we refer to it as DAE. Moreover, right at and immediately after the DAE, a short-lived earthward flow with energetic and thermal ions lasting for ~3 minutes is detected, which manifests a common feature of DAE (see later in Section 4) and is believed to be produced by substorm acceleration at dipolarization [*Shiokawa et al.*, 2005].

4. Statistic Study

[10] This section presents the statistical study of the 53 events. In 36 of these events, plasma data from HIA/TC-1 are available. For 16 events, usable IMAGE/WIC data can be obtained.

4.1. Pileup and DAE

[11] In all 53 events TC-1 first observed a gradual enhancement of B_z and nearly constant B_x, followed by a rapid drop of B_x. A superposed epoch analysis based on all effective events is plotted in Figure 3, which shows that the average properties of pileup and DAE are similar to the characteristic features of 17 September 2004 event. The statistical results can be summarized as follows: (1) Pileup is observed almost simultaneously with aurora breakup within 1–3 minutes and ~11 minutes ahead of the DAE on average. (2) Oscillations of B_z in the Pi2 frequency range start just ahead of pileup, with maximum amplitudes appearing at DAE. (3) The average duration of DAE is about 2 minutes. (4) Among the 36 events for which the HIA/TC-1 data are available, there are 26 in which N_i is reduced during pileup. In 10 cases N_i remains almost unchanged. Besides, in most events β keeps decreasing slightly on average. (5) There are 29 cases in which N_i, T_i and β suddenly jump up right at and immediately after the DAE. In another 7 cases either N_i or T_i rises. (6) In all 36 events earthward flows with speeds ranging from ~50 to ~500 km/s are measured right at the DAE, with a typical duration of ~3 minutes. Note again that in most events the MLTs of TC-1 and auroral breakup are different.

4.2. B_y Changes at the DAE

[12] ΔB_y is found to change sign in most of the 53 events. Table 1 presents the statistical results. It is seen that 40 events with bold numbers are in agreement with the fact that the SCW front, which is 'symmetric' relative to both the central plasma sheet and the Sun-Earth line, is moving across the spacecraft tailward and expanding in the Z-direction right at the DAE. In 10 events the SCW fronts are probably not symmetric so that the opposite situations are obtained.

4.3. TC-1 and Cluster Conjunction

[13] It is worthwhile to note that in 6 cases among 53 events studied, Cluster measured earthward BBFs prior

Table 1. Numbers of Events With Different Signs of ΔB_y Changes at DAE

TC-1 Position[a]	Total Numbers	$\Delta B_y > 0$	$\Delta B_y < 0$	Without Changes
North-Dawn	19	**14**	5	0
North-Dusk	11	3	**7**	1
South-Dawn	16	1	**13**	2
South-Dusk	7	**6**	1	0

[a]TC-1 position relative to the central plasma sheet.

to or during TC-1 flux pileup; while in 5 cases Cluster observe DAE ~10–20 minutes after TC-1. For all these cases the azimuthal angles at the TC-1 and Cluster positions are not too far from each other (with $|\Delta Y_{gsm}| < 4\ R_E$). Since BBFs and SCWs may often be localized in the azimuthal direction, it is not a surprise that not many Cluster/TC-1 conjunctions have been obtained [*Nakamura et al.*, 2006].

5. Discussions and Summary

[14] Flux pileup is clearly seen in 53 substorm events studied in this paper, which is characterized by continuous enhancements of B_z and B_t with the trend of reduction of N_i, P_{th} and β. This is similar to the situation that flux pileup near the subsolar magnetopause squeezes particles out of the compression region, leading to the depletion layer in the adjacent magnetosheath [*Phan et al.*, 1994]. Pileup is observed almost simultaneously with the substorm aurora breakup within 1–3 minutes, indicating that substorm onset is probably in close temporal relation to flow braking and flux pileup. On the other hand, if pileup was observed simultaneously with DAE, the SCW would have already reached the TC-1 position, and the increase in B_z would be due to FACs in the X-direction [*Lopez and Lui*, 1990]. Nevertheless, our observations seem not consistent with this argument.

[15] DAE is also observed at the TC-1 location, which is marked by a sharp drop of B_x and sudden jumps of N_i and T_i, manifesting a rapid expansion of the local plasma sheet. The DAE starts ~11 minutes after the beginning of pileup, implying that at least for the events studied, at the TC-1 location they are two distinct processes. It is likely that high-speed flows stop in the region tailward of TC-1, resulting in an earthward motion of compressed magnetic field and fast-mode waves propagating inward that yield compression of B_z and the related oscillations in Pi2 frequency range. On the other hand, dipolarization originates earthward of TC-1. As the plasma sheet expands, the SCW front moves tailward, TC-1 then observes the drop of B_x, as well as jumps of N_i and T_i when the spacecraft is passing across the boundary to enter the plasma sheet.

[16] In 16 events during which the IMAGE/WIC data are available, IMAGE recorded the aurora brightening in the pre-midnight sector of the southern auroral oval, while TC-1 observations came from the northern/dawnside part of the inner-magnetotail. This is due to the fact that from 20 September to the end of October when the apogee of TC-1 moved to duskside, the IMAGE/WIC data were not available in many substorms. In such a situation accurate timing comparisons between the flux pileup/DAE and auroral breakup are difficult to obtain. Whether the inaccuracy in this aspect makes the results uncertain? Among the 16 events, the cases in which the MLT difference between TC-1 and auroral brightening is less and more than 1 hour are 5 and 11, respectively. Aurora breakups start ~2.2 minutes behind pileup for the former and ~2.7 minutes for the latter on average. No significant difference is seen. Meanwhile, in a half of events aurora breakup appears just on the westward side of TC-1 within 2 hours of MLT, which is expectable if the SCW forms in association with pileup. Furthermore, in the 5 and 11 events for which the MLT difference between TC-1 and auroral brightening is, respectively, less and more than 1 hour, DAE occurs ~8 and ~9 minutes later than aurora breakup, respectively. Again no significant difference is found. The SCW expands both radially and azimuthally during the expansion phase [*Lopez and Lui*, 1990]. If DAEs were essentially due to the azimuthal expansion, the spacecraft would see a clear jump in B_z. Both Figures 1 and 3 do not show this feature. The fact that the B_y changes are consistent to dawn/dusk location of the satellite implies that DAEs may mainly be attributed to the radial expansion/tailward propagation of SCW, associated with an expansion in the Z-direction. In short, the main results of observations (i.e., substorm onset is in close relation to flux pileup and the SCW first forms earthward of the flow braking region) seem to be reliable, though in most events the MLTs of TC-1 and auroral breakup are seemly different.

[17] To understand the above results, we first recall the 3-D MHD simulation of substorm current wedge formation by *Birn et al.* [1999]. It is shown that flow braking maximizes at $X \approx -15\ R_E$, while current diversion takes place mostly earthward of $X \approx -12\ R_E$, in association with drastic reduction of the curvature drift current due to an expansion of the plasma sheet. Alternatively, flow braking might yield favorable conditions for instabilities to grow near the inner edge of the plasma sheet, which ultimately lead to dipolarization at substorm onset [*Pu et al.*, 2001]. In addition, tailward flows of ionospheric origin are often observed by TC-1 prior to the expansion onset. It is suggested that the interaction of the tailward flows with earthward BBFs might also contribute to the substorm triggering [*Liu et al.*, 2006]. Global/multiscale substorm initiation processes should be considered.

[18] In summary, 53 substorm events measured by Double Star/TC-1 from July to October, 2004 are studied. Magnetic flux pileup is directly observed in all events, which starts almost simultaneously, 1–3 minutes, with the aurora breakup, indicating that substorm onset is in close temporal relation to flow braking and flux pileup. DAE also occurs in all events, which is observed ~11 minutes after the beginning of pileup. There is evidence that the SCW first forms earthward of TC-1 and, hence, inward the flow braking region and then propagates tailward with an expansion in the Z-direction. The initial location, formation and propagation/expansion of SCW desire further studies.

[19] **Acknowledgments.** This work is supported by the NSFC grants (40390152, 40536030, 40425004, 40528005 and 40374061) and Chinese Key Research Project (grant 2006CB806300), as well as the Chinese Double Star-Cluster Science Team. The authors acknowledge CNSA and ESA for the successful Double Star Mission, PPARC for supporting the operations of the FGM instruments, and ACE/MAG team for IMF data. We also appreciate the useful discussions with R. L. McPherron, A. T. Y. Lui and R. Nakamura. The authors particularly thank two reviewers for their pertinent and constructive comments and suggestions.

References

Baker, D. N., et al. (1996), Neutral line model of substorms: Past results and present view, *J. Geophys. Res.*, *101*(A6), 12,975–13,010.

Baumjohann, W. (2002), Modes of convection in the magnetotail, *Phys. Plasmas*, *9*(9), 3665–3667, doi:10.1063/1.1499116.

Baumjohann, W., et al. (1999), Substorm dipolarization and recovery, *J. Geophys. Res.*, *104*(A11), 24,995–25,000.

Birn, J., M. Hesse, G. Haerendel, W. Baumjohann, and K. Shiokawa (1999), Flow braking and the substorm current wedge, *J. Geophys. Res.*, *104*(A9), 19,895–19,904.

Carr, C., et al. (2005), The Double Star magnetic field investigation: Instrument design, performance and highlights of the first year's observations, *Ann. Geophys.*, *23*, 2713–2732.

Fazakerley, A. N., et al. (2005), The Double Star plasma electron and current experiment, *Ann. Geophys.*, *23*, 2733–2756.

Frey, H. U., S. B. Mende, V. Angelopoulos, and E. F. Donovan (2004), Substorm observations by IMAGE-FUV, *J. Geophys. Res.*, *109*, A10304, doi:10.1029/2004JA010607.

Jacquey, C., J. A. Sauvaud, and J. Dandouras (1991), Location and Propagation of the magnetotail current disruption during substorm expansion: Analysis and simulation of an ISEE multi-onset event, *Geophys. Res. Lett.*, *18*(3), 389–392.

Liu, Z. X., et al. (2005), The Double Star mission, *Ann. Geophys.*, *23*, 2707–2712.

Liu, Z. X., et al. (2006), Global and multi-scale processes of magnetospheric substorm driven and trigger: 'SymmetricFront model' of substorm trigger, paper presented at 2006 Assembly, Comm. on Space Res. (COSPAR), Beijing.

Lopez, R. E., and A. T. Y. Lui (1990), A multisatellite case study of the expansion of a substorm current wedge in the near-Earth magnetotail, *J. Geophys. Res.*, *95*(A6), 8009–8017.

Lui, A. T. Y. (1996), Current disruption in the Earth's magnetosphere: Observations and models, *J. Geophys. Res.*, *101*, 13,067–13,088.

McPherron, R. L. (1991), Physical processes producing magnetospheric substorms and magnetic storms, in *Geomagnetism*, vol. 4, edited by J. A. Jacobs, pp. 593–739, Elsevier, New York.

Nagai, T., et al. (1998), Structure and dynamics of magnetic reconnection for substorm onsets with Geotail observations, *J. Geophys. Res.*, *103*(A3), 4419–4440.

Nakamura, R., et al. (2006), Fast flow, dipolarization, and substorm evolution: Cluster/Double Star multipoint observations, in *ISC-8 Proc.*, edited by E. Donovan, Natl. Res. Counc. of Can., Ottawa, Ont., Canada, in press.

Phan, T. D., et al. (1994), The magnetosheath region adjacent to the dayside magnetopause: AMPTE/IRM observations, *J. Geophys. Res.*, *99*(A1), 121–142.

Pu, Z. Y., et al. (2001), A Global synthesis model of dipolarization at substorm expansion onset, *J. Atmos. Solar Terr. Phys.*, *63*, 671–681.

Rème, H., et al. (2005), The HIA instrument on board the Tan Ce 1 Double Star near-equatorial spacecraft and its first results, *Ann. Geophys.*, *23*, 2757–2774.

Shiokawa, K., W. Baumjohann, and G. Haerendel (1997), Braking of high-speed flows in the near-Earth tail, *Geophys. Res. Lett.*, *24*(10), 1179–1182.

Shiokawa, K., et al. (1998), High-speed ion flow, substorm current wedge, and multiple Pi2 pulsations, *J. Geophys. Res.*, *103*(A3), 4491–4507.

Shiokawa, K., et al. (2005), Decrease in B_z prior to the dipolarization in the near-Earth plasma sheet, *J. Geophys. Res.*, *110*, A09219, doi:10.1029/2005JA011144.

W. Baumjohann, Space Research Institute, Austrian Academy of Sciences, Schmiedlstr. 6, A-8042 Graz, Austria. (baumjohann@oeaw.ac.at)

J. B. Cao and Z. X. Liu, Center for Space Science and Applied Research, PO Box 8701, 100080 Beijing, China. (liu@center.cssar.ac.cn; jbcao@center.cssar.ac.cn)

X. Cao, S. Y. Fu, Z. Y. Pu, and H. Zhang, School of Earth and Space Sciences, Peking University, Beijing 100871, China. (cx_octor@pku.edu.cn; suiyanfu@pku.edu.cn; zypu@pku.edu.cn; hui@pku.edu.cn)

C. Carr, Space and Atmospheric Physics Group, Blackett Laboratory, Imperial College, Prince Consort Road, London SW7 2BZ, UK. (c.m.carr@ic.ac.uk)

I. Dandouras and H. A. Rème, CESR/CNRS, 9 Avenue du Colonel Roche, B.P. 4346, F-31028 Toulouse, France. (iannis.dandouras@cesr.fr; henri.reme@cesr.fr)

M. W. Dunlop, Rutherford Appleton Laboratory, Chilton, Didcot, Oxon OX11 0QX, UK. (m.dunlop@rl.ac.uk)

C. P. Escoubet, ESA/ESTEC (SCI-RSSD), Postbus 299, Keplerlaan, 1, NL-2200 AG Noordwijk, Netherlands. (philippe.escoubet@esa.int)

A. Fazakerley, Department of Physics, Mullard Space Science Laboratory, University College London, Holmbury St. Mary, Dorking, Surrey, RH5 6NT, UK. (anf@mssl.ucl.ac.uk)

H. U. Frey, Space Sciences Laboratory, University of California, 7 Gauss Way, Berkeley, CA 94720-7450, USA. (hfrey@ssl.berkeley.edu)

M. H. Hong, Institute of Geology and Geophysics, CAS, 100029, Beijing, China. (mhhong@mail.c-geos.ac.cn)

Z. W. Ma, Department of Physics, Zhejiang University, 310027, Hangzhou, China. (zwma@zju.edu.cn)

X. G. Wang, School of Physics, Peking University, 100871, Beijing, China. (xgwang@pku.edu.cn)

C. J. Xiao, National Astronomical Observatories, CAS, 100012, Beijing, China. (cjxiao@ourstar.bao.ac.cn)

Q. G. Zong, Center for Atmospheric Research, University of Massachusetts Lowell, 600 Suffolk Street, Lowell, MA 01854-3629, USA. (qiugang_zong@uml.edu)